LA-UR-16-29373
Approved for public release; distribution is unlimited.

Title: The Impact of Data Shortfalls on Reliability Uncertainty: Using the Rationale for Assessing Degradation Arriving at Random Methodology

Author(s): Hamada, Michael Scott
Abes, Jeff I.
Hills, Charles Robert

Intended for: Report

Issued: 2016-12-13

The Impact of Data Shortfalls on Reliability Uncertainty: Using the Rationale for Assessing Degradation Arriving at Random Methodology

J. I. Abes
Surveillance Oversight
Los Alamos National Laboratory

M. S. Hamada
Statistical Sciences
Los Alamos National Laboratory

C. R. Hills
Surveillance Oversight
Los Alamos National Laboratory

12.01.16 1600

Abstract

The impact of data shortfalls on reliability uncertainty is studied using the Rationale for Assessing Degradation Arriving at Random (RADAR) Bayesian methodology for a series system.

Key Words: Bayesian inference, RADAR methodology, series system, system reliability.

1 Introduction

This article proposes using the RADAR methodology (a Rationale for Assessing Degradation Arriving at Random (Vander Wiel et al. (2011)) to assess the impact of nuclear weapon surveillance data shortfalls on reliability uncertainty. The RADAR approach provides an advantageous alternative to the look-back period methodology proposed in Hamada et al. (2015).

An outline of this article is as follows. First, we review the RADAR methodology. Then, we apply the RADAR methodology to a system consisting of six subsystems in series. Next, we consider the impact of data shortfalls when testing ceases or is stopped. Finally, we conclude with a discussion.

Consider a system like the NEP with six subsystems: GTS, DET, HE, PIT, CASE, CSA. There are multiple diagnostics applied in surveilling each subsystem. In this article, we will summarize all these results as a pass or fail for each of the subsystems. A pass or fail does not necessarily mean that the system will work or not but we treat them as such to assess reliability uncertainty. In fact, we consider the scenario in which the surveillance data lead to passes for all subsystems.

The number and frequency of surveillance can differ by subsystem, say, seven a year for DET and one every three years for CSA. Note that these data counts and any others used in this article are for illustrative purposes only.

Here, we consider a series system in which all the subsystems have to work in order for the system to work. For a series system and assuming that the subsystems act independently, the system reliability is the product of the subsystem reliabilities. As discussed above, we will use pass/fail data to assess reliability and use a Bayesian approach to obtain a posterior distribution on subsystem reliability. We can then randomly sample from each of these subsystem reliability distributions and multiply them together to obtain a random sample from the system reliability distribution. Here we use the 90% lower bound known as the 90% credible lower bound to assess reliability uncertainty; that is, we are 90% confident that the reliability exceeds this lower bound.

2 The RADAR Methodology

Vander Wiel et al. (2011) propose the RADAR methodology with the following prior model for reliability over time. Let π_t be the reliability at year t that is defined as follows:

$$\begin{aligned} \pi_0 &= \rho_0, \\ \pi_t &= \rho_t \pi_{t-1}, t = 1, 2, \ldots, \end{aligned} \tag{1}$$

where the annual degradation rate ρ_t is defined as

$$\begin{aligned} \rho_t &= r_t, t = 0, 1 \\ \rho_t &= r_t \rho_{t-1}, t = 2, 3, \ldots. \end{aligned} \tag{2}$$

Moreover, independent shocks r_t are distributed as $r_t \sim OneBeta(p_t, a_t, b_t)$, where the One-Beta distribution is defined as

$$\begin{aligned} &1 \text{ with probability } p_t, \\ &Beta(a_t, b_t), \text{otherwise.} \end{aligned} \tag{3}$$

That is, with probability p_t, the shock r_t is less than 1 drawn from a $Beta(a_t, b_t)$ distribution. Equation (2) implies that this less than one shock r_t is applied in year t and every year thereafter. Here, we use $(a_0, b_0, p_0) = (99, 1, 0.5)$ and $(a_t, b_t, p_t) = (99, 1, 0.98)$ that Vander Wiel et al. (2011) used in their examples.

Figure 1 shows the 0.5, 0.25, 0.10 quantiles of prior π_t over 25 years for $(a_t, b_t, p_t) = (99, 1, 0.98)$.

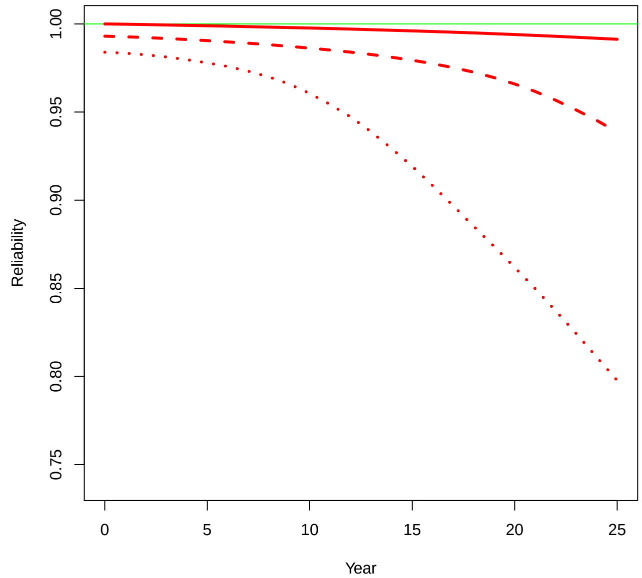

Figure 1: Prior π_t 0.5, 0.25, 0.10 quantiles over 25 years for $(a_0, b_0, p_0) = (99, 1, 0.5)$ and $(a_t, b_t, p_t) = (99, 1, 0.98)$.

Now consider the data collected over time. Let X_t for $t = 0, \ldots, T$ denote the number of passes out of n_t tests. Here, we assume all passes, so that $X_t = n_t$. Further, we let the collection of data through the Tth year be denoted by S_T, where $S_T = \{X_t = n_t, t = 0, \ldots, T\}$. Also, let $N_{0:T} = \sum_{i=0}^{T} n_t$ and $N_{t:T} = \sum_{i=t}^{T} (i - t + 1) n_t$.

Then, Vander Wiel et al. (2011) show that the posterior r_t also has a OneBeta distribution:

$$r_t | S_T \sim OneBeta(p'_{t,T}, at + N_{t:T}, b_t), \tag{4}$$

where

$$p'_{t,T} = \frac{p_t B(a_t, b_t)}{p_t B(a_t, b_t) + (1 - p_t) B(a_t + N_{t:T}, b_t)} \tag{5}$$

and $B(a, b) = \frac{\Gamma(a)\Gamma(b)}{\Gamma(a+b)}$. Then the posterior π_t can be expressed as $\pi_t = r_0 \prod_{i=1}^{T} r_i^{t-i+1}$. For $t > T$, r_t still has its prior distribution because r_t is independent of S_T. The independence no longer holds if there is at least one fail; see Vander Wiel et al. (2011) for details.

3 Results for Two Scenarios

Suppose that for (GTS, DET, HE, PIT, CASE) subsystems, n_t tests are (4, 7, 4, 1, 1) up to $T = 10$ and for the CSA subsystem $n_0 = 1$ and then 1 test every three years so that there are a total of 4 tests at $T = 10$, i.e., the sequence is (1, 0, 0, 1, 0, 0, 1, 0, 0, 1, 0). We also consider $T = 20$ so that for the CSA subsystem, there is a total of 7 tests at $T = 20$.

We use the reliability prior in Figure 1 and apply the RADAR methodology to obtain posterior reliabilities whose 0.5, 0.25, 0.10 quantiles are plotted in Figure 2 for GTS and HE, Figure 3 for DET, Figure 4 for PIT and CASE and Figure 5 for CSA for the scenario $T = 10$. The posterior quantiles appear as black lines. The prior quantiles appear as red lines. The green line corresponds to a reliability of 1 for reference. For the scenario $T = 20$, the corresponding figures are Figures 6-9.

Note that all the S_T data are being used to update all the reliabilities. That is, this is what we know based on the data at $T = 10$ or $T = 20$.

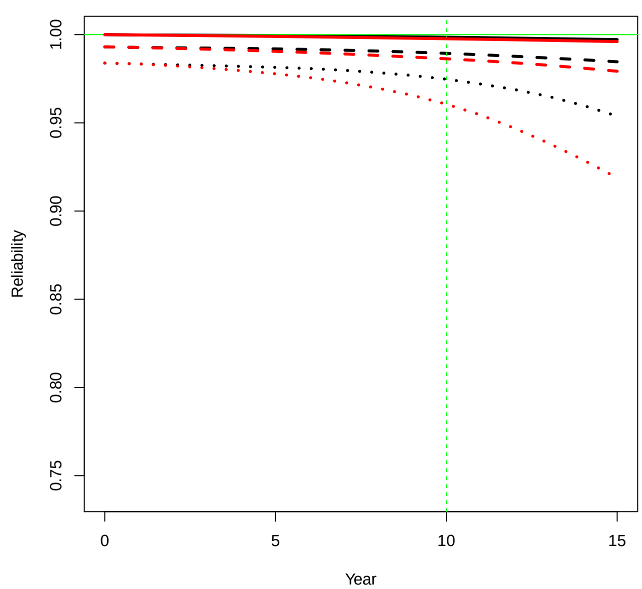

Figure 2: Reliability prior and posterior 0.5, 0.25, 0.10 quantiles for GTS and HE subsystems for the scenario $T = 10$. The black and red lines correspond to posterior and prior quantiles, respectively.

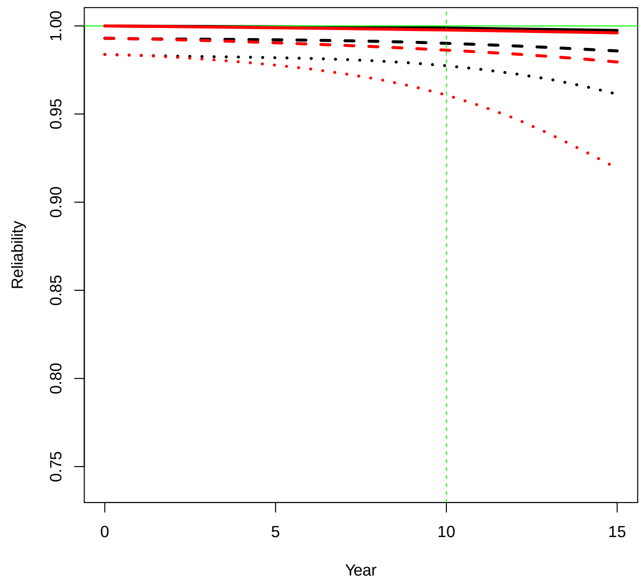

Figure 3: Reliability prior and posterior 0.5, 0.25, 0.10 quantiles for DET subsystem for the scenario $T = 10$. The black and red lines correspond to posterior and prior quantiles, respectively.

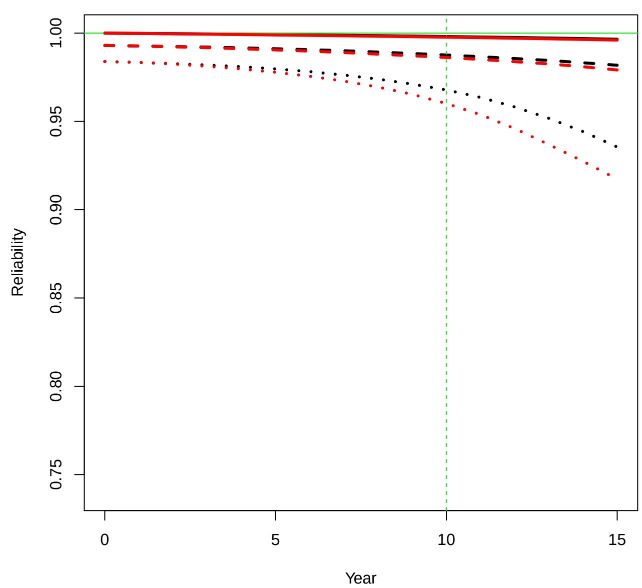

Figure 4: Reliability prior and posterior 0.5, 0.25, 0.10 quantiles for PIT and CASE subsystems for the scenario $T = 10$. The black and red lines correspond to posterior and prior quantiles, respectively.

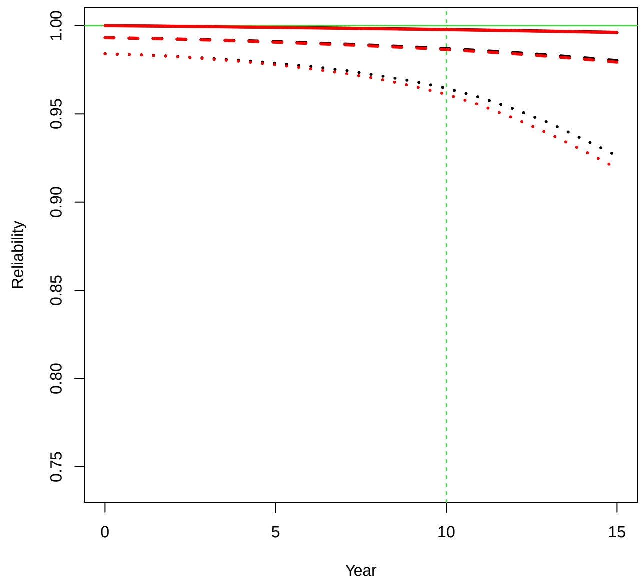

Figure 5: Reliability prior and posterior 0.5, 0.25, 0.10 quantiles for CSA subsystem for the scenario $T = 10$. The black and red lines correspond to posterior and prior quantiles, respectively.

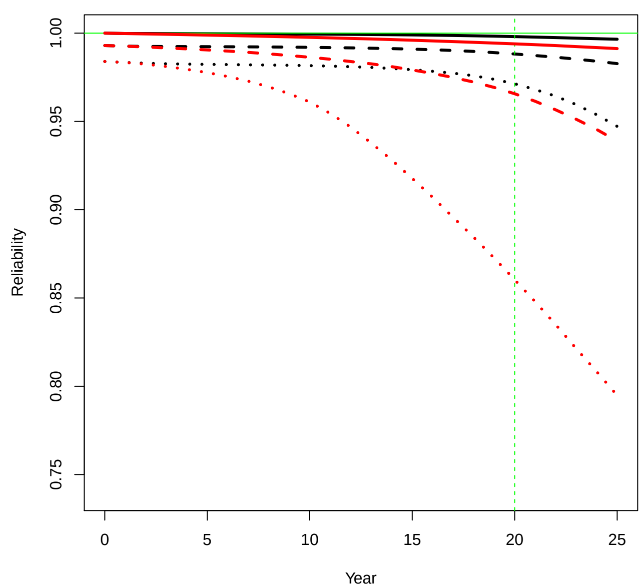

Figure 6: Reliability prior and posterior 0.5, 0.25, 0.10 quantiles for GTS and HE subsystems for the scenario $T = 20$. The black and red lines correspond to posterior and prior quantiles, respectively.

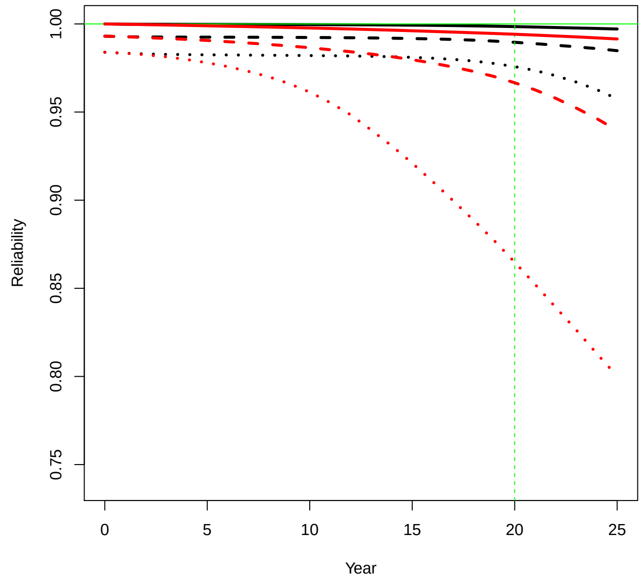

Figure 7: Reliability prior and posterior 0.5, 0.25, 0.10 quantiles for DET subsystem for the scenario $T = 20$. The black and red lines correspond to posterior and prior quantiles, respectively.

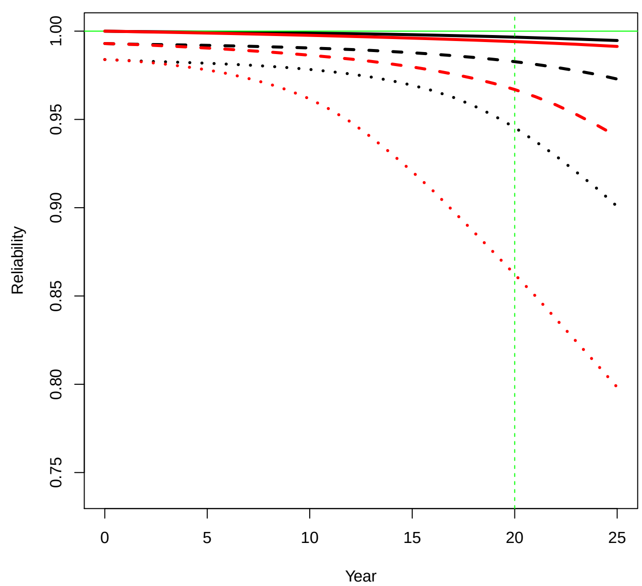

Figure 8: Reliability prior and posterior 0.5, 0.25, 0.10 quantiles for PIT and CASE subsystems for the scenario $T = 20$. The black and red lines correspond to posterior and prior quantiles, respectively.

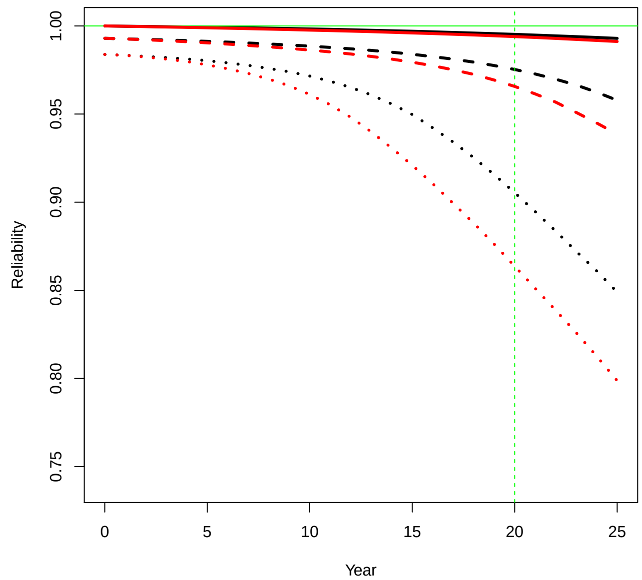

Figure 9: Reliability prior and posterior 0.5, 0.25, 0.10 quantiles for CSA subsystem for the scenario $T = 20$. The black and red lines correspond to posterior and prior quantiles, respectively.

To illustrate how we obtain the system reliability posterior, we show the reliability posteriors of the subsystems in Figures 10 and 12 at $T = 10$ or $T = 20$, respectively. The 90% credible lower bounds on reliability appear as dashed lines. As discussed in the Introduction, the posterior system reliability distribution can be sampled by sampling all the posterior subsystem reliability distributions and multiplying the subsystem reliabilities to obtain a system reliability for a series system. The reliability posteriors for the systems are shown in Figures 11 and 13 at $T = 10$ and $T = 20$, respectively. We see that although the subsystem posteriors in Figures 10 and 12 increase monotonically, the series system posteriors in Figures 11 and 13 do not with their peaks occurring at a reliability less than one.

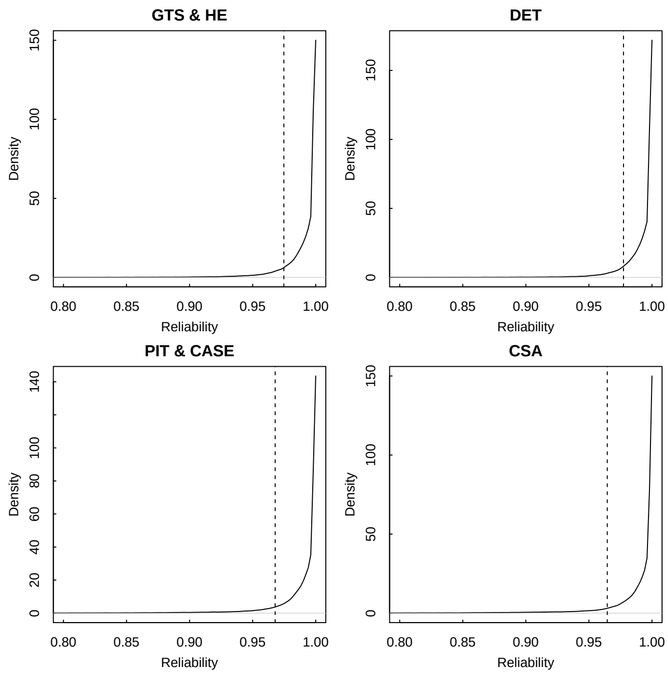

Figure 10: Posterior Distribution of Subsystem Reliability at $T = 10$ (90% credible lower bound as dashed line)

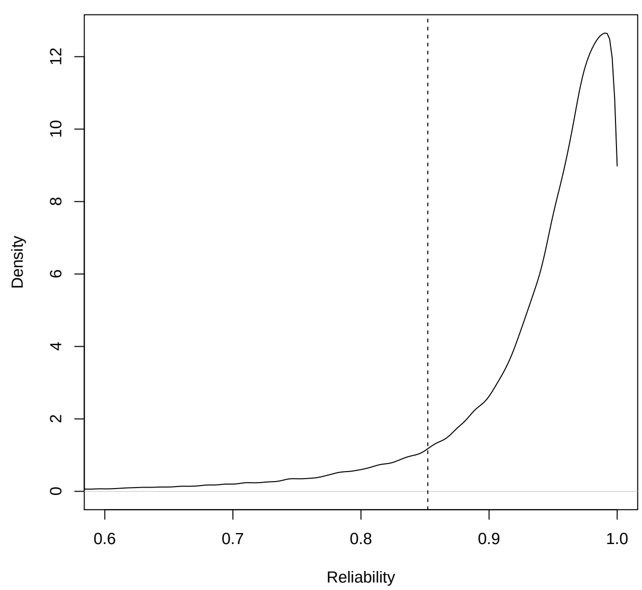

Figure 11: Posterior Distribution of System Reliability at $T = 10$ (90% credible lower bound as dashed line)

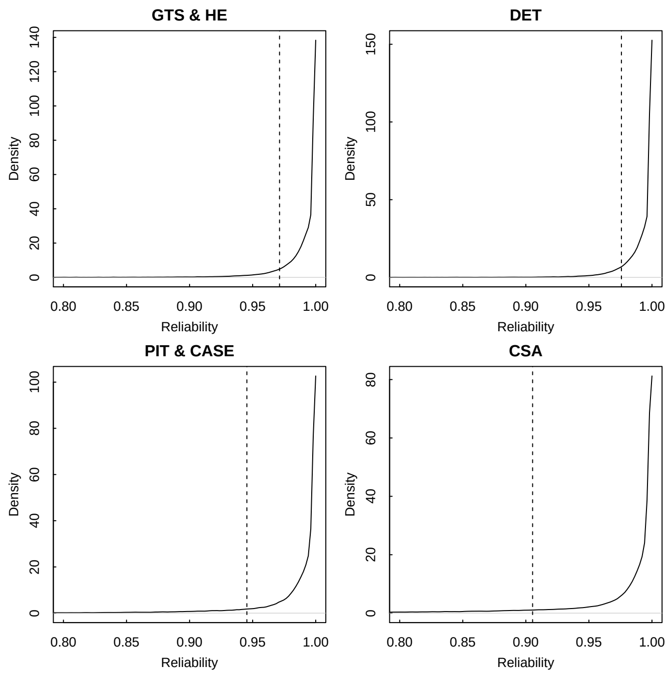

Figure 12: Posterior Distribution of Subsystem Reliability at $T = 20$ (90% credible lower bound as dashed line)

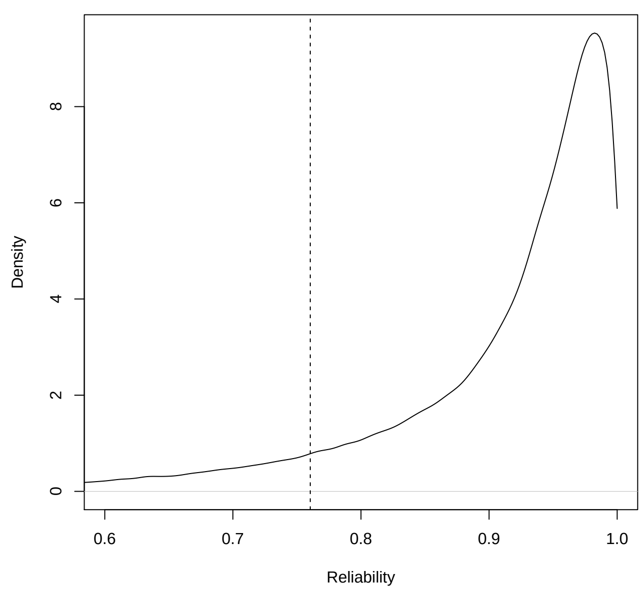

Figure 13: Posterior Distribution of System Reliability at $T = 20$ (90% credible lower bound as dashed line)

The posterior system reliabilities whose 0.5, 0.25, 0.10 quantiles are plotted in Figures 14 and 15 for $T = 10$ and $T = 20$, respectively, and correspond to the subsystem plots in Figures 2-5 and Figures 6-9 for $T = 10$ and $T = 20$, respectively.

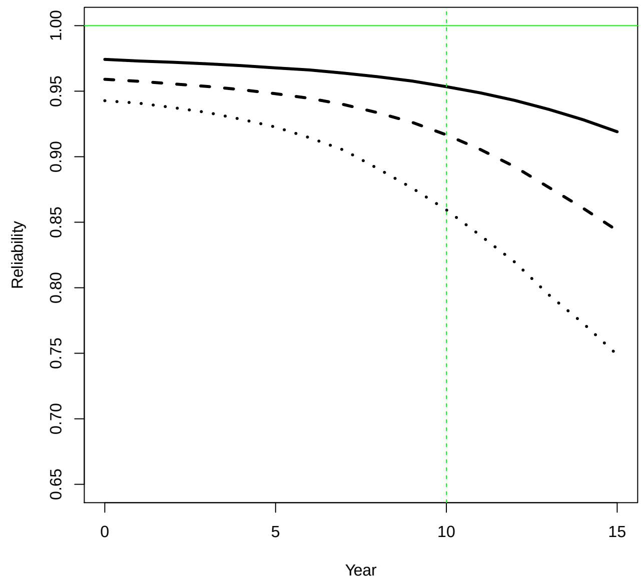

Figure 14: Reliability prior and posterior 0.5, 0.25, 0.10 quantiles for system for the scenario $T = 10$.

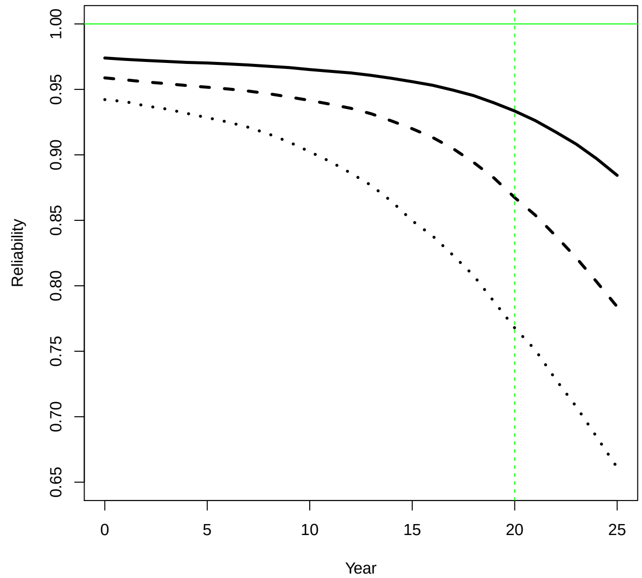

Figure 15: Reliability prior and posterior 0.5, 0.25, 0.10 quantiles for system for the scenario $T = 20$.

Based on this method, as shown by Figure 2, a reasonable sampling frequency maintains a high credible lower bound for component reliability. There is a point of diminishing returns for sampling frequency, as shown by comparing Figure 3 to Figure 2. For very low sampling frequencies, the credible lower bound for component reliability can start to plummet, as shown by Figure 9. When only examining results for individual components, this might not seem too bad at first, given that the lowest 90% credible lower bound shown in Figure 12 is still above 0.9. The component results are multiplied together to produce the credible lower bound for the system, however, and the 90% credible lower bound shown in Figure 13 is below 0.8, which indicates that sampling frequency matters: the sampling rates for the CSA, PIT, and CASE are indeed too low.

4 Illustrating the Impact of Data Shortfalls

Suppose that we stop testing at $T = 10$ or $T = 20$ and consider the impact of no testing for 5 years after T. We summarize the 0.10 quantile of posterior reliability for the subsystems and system in Tables 1 and 2 for $T = 10$ and $T = 20$, respectively. Figure 16 displays the system reliability uncertainty for 0-5 years of data shortfalls for $T = 10$ (solid) and $T = 20$ (dashed). We see that the system reliability uncertainty is much more at $T = 20$ than at $T = 10$, i.e., before any data shortfall. This feature illustrates that even though we have an additional 10 years of testing at the same rates, even more data is needed as a system ages to maintain the same uncertainty. Figure 16 shows that data shortfalls have a significant effect. The system 90% credible lower bound falls by more than 0.10 probability (i.e., 10 percentage points) in 5 years.

Table 1: Impact of Data Shortfalls for $T = 10$ on Reliability Uncertainty (90% credible lower bound)

	Number of Shortfall Years					
	0	1	2	3	4	5
GTS	0.975	0.972	0.969	0.965	0.960	0.954
DET	0.977	0.975	0.973	0.970	0.966	0.961
HE	0.975	0.972	0.969	0.965	0.960	0.954
PIT	0.968	0.964	0.958	0.952	0.944	0.936
CASE	0.968	0.964	0.958	0.952	0.944	0.936
CSA	0.965	0.959	0.953	0.945	0.936	0.926
SYSTEM	0.859	0.840	0.820	0.795	0.773	0.749

Table 2: Impact of Data Shortfalls for $T = 20$ on Reliability Uncertainty (90% credible lower bound)

	Number of Shortfall Years					
	0	1	2	3	4	5
GTS	0.971	0.968	0.964	0.960	0.954	0.947
DET	0.976	0.974	0.971	0.967	0.963	0.958
HE	0.971	0.968	0.964	0.960	0.954	0.947
PIT	0.945	0.938	0.929	0.920	0.911	0.901
CASE	0.945	0.938	0.929	0.920	0.911	0.901
CSA	0.905	0.895	0.884	0.872	0.861	0.849
SYSTEM	0.768	0.751	0.729	0.708	0.685	0.661

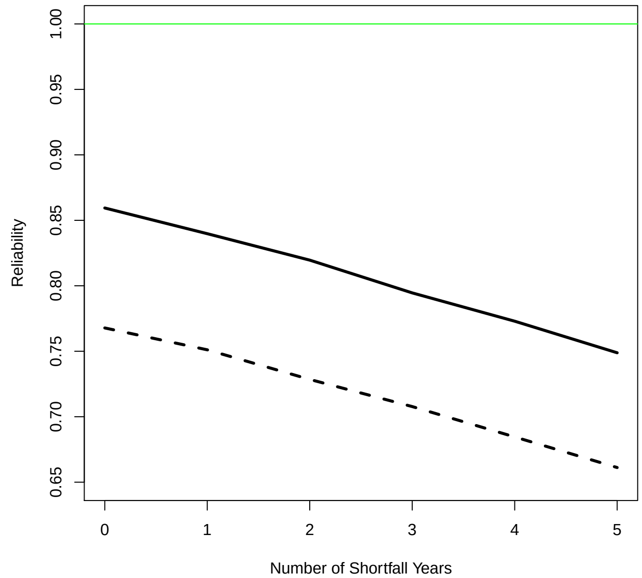

Figure 16: Impact of Data Shortfalls on System Reliability Uncertainty (solid and dashed are for $T = 10$ and $T = 20$).

5 Discussion

In this article, we showed how the impact of data shortfalls on reliability uncertainty can be assessed. While quantitative, it provides a qualitative feel the impact on the actual reliability uncertainty; recall that all the surveillance data on a subsystem are being assessed as a pass or fail. Moreover, if an abnormal observation arises in surveillance, it is the SFI process that determines whether reliability is impacted and to what degree. In this article, the numbers used are illustrative. Other scenarios with different numbers and frequency can easily be assessed.

The challenge will be to develop criteria for how to communicate uncertainty on reliability to the assessment community and how or if we use uncertainty on reliability in reporting reliability.

References

Hamada, M.S., Hills, C.S., and Abes, J.I. (2015). The Impact of Data Shortfalls on Reliability Uncertainty. Los Alamos National Laboratory Technical Report W-9-TR-O285U(A).

Hamada, M.S., Wilson, A.G., Reese, C.S., and Martz, H.F. (2008). *Bayesian Reliability*, Springer, New York.

Vander Wiel, S., Wilson, A., Graves, T. and Reese, S. (2011). A Random Onset Model for Degradation of High-Reliability Systems. *Technometrics*, 53, 163-172.